Supplemental material

Computational material screening for electrode materials of $BaSi_2$ solar cells

Tomoaki Yazaki[a], Keisuke Arimoto[a], Junji Yamanaka[a], and Kosuke O. Hara[b]

[a]University of Yamanashi, 7-32 Miyamae, Kofu, Yamanashi, Japan

[b]Nara Institute of Science and Technology, 8916-5 Takasyama, Ikoma, 630-0192, Nara, Japan

1. Data list of work functions

Table S1 lists the work functions of elemental metals estimated by the density functional theory (DFT) calculations and the machine learning model [S1] together with reference values [S2].

Table S1 Work functions of elemental metals estimated by DFT calculations and the machine learning model [S1] together with reference values [S2]. Estimations are for (100) orientations. Reference values are for (100) if available; otherwise, for polycrystalline samples.

Formula	Work function (DFT) [eV]	Work function (machine learning) [eV]	Work function (reference [S2]) [eV]
Ag	4.39	4.22	4.64
Al	4.38	4.25	4.2
Au	5.23	4.90	5.47
Ba	2.40	2.33	2.52
Be	3.93	3.86	4.98
Ca	2.76	2.79	2.87
Cs	1.99	2.01	1.95
Cu	4.65	4.61	5.1
Ga	4.37	4.33	4.32
Hf	3.69	3.57	3.9

In	3.95	4.01	4.09
K	2.22	2.38	2.29
Li	3.06	3.01	2.93
Mg	3.69	3.51	3.66
Mo	3.98	4.00	4.53
Na	2.66	2.83	2.36
Nb	3.67	3.75	4.02
Os	4.89	4.81	5.93
Pb	3.85	3.94	4.25
Pd	5.23	5.03	5.22
Pt	5.81	5.59	5.64
Rb	2.17	2.21	2.261
Re	4.52	4.42	4.72
Rh	5.23	4.96	4.98
Ru	4.60	4.44	4.71
Sc	3.32	3.23	3.5
Sn	4.27	4.29	4.42
Ta	3.90	4.22	4.15
Ti	3.70	3.49	4.33
V	3.84	4.00	4.3
W	4.21	4.36	4.63
Zn	4.60	4.07	3.63
Zr	3.68	3.41	4.05

2. Validation of the screening workflow on pn-junction Si solar cells

To validate our screening workflow, we searched for electrode materials for pn-junction crystalline Si solar cells. The device model for simulations consisted of an n-type Si layer (100 nm) on the top side and a p-type Si layer (200 μm) on the bottom side. The electron and hole concentrations in the n- and p-type layers were 1×10^{19} cm^{-3} and 1×10^{16} cm^{-3}, respectively. The permittivity, bandgap, electron affinity, effective density of states of the conduction band, effective density of states of the valence band, electron mobility, and hole mobility were 11.9, 1.12 eV, 4.05 eV, 2.86×10^{19} cm^{-3}, 2.66×10^{19} cm^{-3}, 1450 $cm^2/V\cdot s$, and 505 $cm^2/V\cdot s$, respectively, according to ref. [S3]. The optical absorption coefficients were taken from ref. [S4]. Because wxAMPS does not accept Auger recombination coefficients, acceptor-type midgap defects were assumed to simulate realistic Si materials. We assumed the density, energy level, and capture cross section to be 1×10^{12} cm^{-3}, 0.56 eV, and 1×10^{-16} cm^2, respectively. This led to a carrier lifetime of approximately 1 ms. The simulation temperature was 300 K, and the effective surface recombination speed was 1×10^{7} cm/s. The top and bottom reflectances were 0 and 1,

respectively.

Figure S1 shows the power conversion efficiency of the pn-junction Si solar cells as functions of the work functions of the bottom and top electrodes. These results indicate the range of work functions that yield high power conversion efficiency: Specifically, ≥ 5.45 eV for the bottom electrode and ≤ 3.65 eV for the top electrode.

Then, computational material screening was performed. For the validation, the search space was confined to elements excluding noble gases, radioactive elements, and actinoids. The melting point threshold was set to 300 K. Table S2 summarizes the candidate materials in descending order of electrical conductivity (accurately, electrical conductivity divided by the relaxation time. Please see the main text for details). Work function criteria were not considered to prepare this table. If we apply the work function criteria, only Na remains as a candidate. However, Na is highly reactive with air and is therefore not used in practical solar cells. Additionally, a common approach is to heavily dope with impurities to avoid the effect of Fermi level pinning and form ohmic contacts on Si by taking advantage of its excellent dopability. Therefore, ignoring the work function criterion aligns with the design concept of practical Si solar cells. However, if we consider other semiconductors that do not significantly suffer from Fermi level pinning, the work function criteria would be useful for effective screening. Table S2 shows that Al, In, Ag, etc. are promising candidates. This result agrees with the electrode materials (Al and Ag) used in practical Si solar cells [S5]. In is avoided probably because of its low melting point, scarcity of resources, and high cost. Thus, our screening workflow has been shown to reach practical electrode materials for crystalline Si solar cells.

Figure S1 Power conversion efficiency of pn-junction solar cells simulated by wxAMPS as functions of work function of (a) bottom and (b) top electrodes.

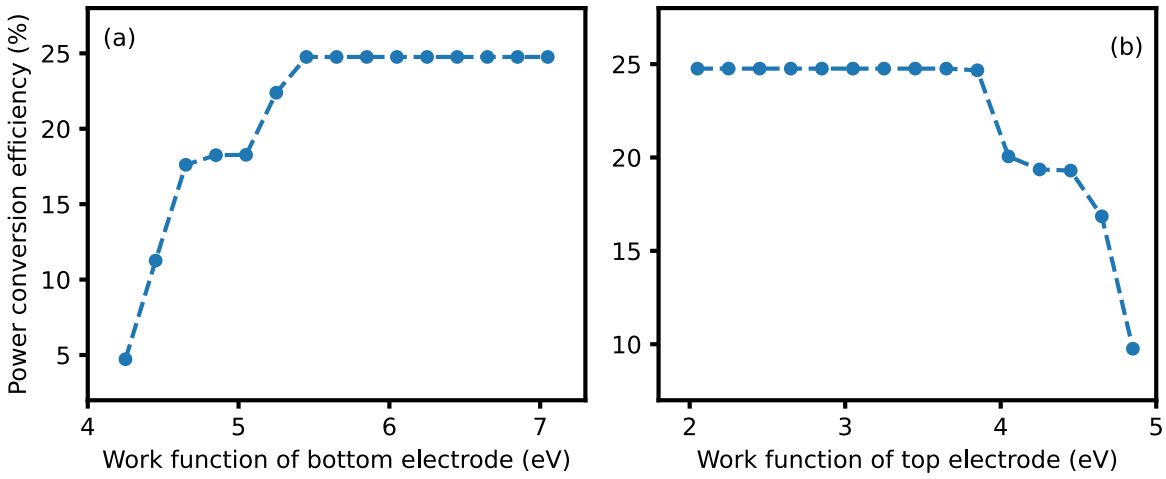

Table S2 List of elements that passed computational material screening. The considered criteria included bandgap, phase stability, interface reactivity, and melting point. The estimated work function is also listed, but was not used for screening. The elements are listed in descending order of electrical

conductivity divided by the relaxation time.

Formula	mp-ID	Melting point (K)	Work function (eV)	Electrical conductivity (S/cm·s)
Al	mp-134	991	4.19	3.13×10^{6}
In	mp-85	404	4.05	1.99×10^{6}
Ag	mp-8566	1208	4.19	1.66×10^{6}
Zn	mp-79	647	4.03	1.65×10^{6}
Pb	mp-20483	566	3.96	1.64×10^{6}
Au	mp-81	1277	4.87	1.56×10^{6}
Cd	mp-94	617	3.93	1.23×10^{6}
Tl	mp-82	562	3.81	1.04×10^{6}
Na	mp-10172	350	2.80	7.29×10^{5}
Be	mp-87	1542	4.46	7.22×10^{5}
Ga	mp-142	314	4.29	5.40×10^{5}
Sb	mp-104	853	4.70	2.82×10^{4}
Sn	mp-117	503	4.29	2.71×10^{4}
Ge	mp-32	1176	4.74	1.76×10^{3}

References

[S1] Schindler P, Antoniuk ER, Cheon G, et al. Discovery of stable surfaces with extreme work functions by high-throughput density functional theory and machine learning. Adv Funct Mater. 2024;34(19): 2401764.

[S2] Lide DR, editor. CRC handbook of chemistry and physics, internet version 2005. CRC press; 2005.

[S3] Sze SM., Semiconductor Devices: Physics and Technology, 2nd Edition. John Wiley & Sons. Inc.; 2002, translated by YNannichi Y, Kawabe M, and Hasegawa F, Japan UNI Agency, Inc.; 2004.

[S4] Green MA and Keevers M, Optical properties of intrinsic silicon at 300 K, Prog Photovolt. 1995;3:189.

[S5] Avrutin V, Izyumskaya N, and Morkoç H, Semiconductor solar cells: Recent progress in terrestrial applications. Superlattices Microstruct. 2011;49:337.